

Time-frequency dynamics of superluminal pulse transition to the subluminal regime

Ahmed H. Dorrah, Abhinav Ramakrishnan, and Mo Mojahedi

Edward S. Rogers Sr. Department of Electrical and Computer Engineering, University of Toronto, Toronto, Ontario M5S 3G4, Canada

(Received 1 December 2014; published 24 March 2015)

Spectral reshaping and nonuniform phase delay associated with an electromagnetic pulse propagating in a temporally dispersive medium may lead to interesting observations in which the group velocity becomes superluminal or even negative. In such cases, the finite bandwidth of the superluminal region implies the inevitable existence of a cutoff distance beyond which a superluminal pulse becomes subluminal. In this paper, we derive a closed-form analytic expression to estimate this cutoff distance in abnormal dispersive media with gain. Moreover, the method of steepest descent is used to track the time-frequency dynamics associated with the evolution of the center of mass of a superluminal pulse to the subluminal regime. This evolution takes place at longer propagation depths as a result of the subluminal components affecting the behavior of the pulse. Finally, the analysis presents the fundamental limitations of superluminal propagation in light of factors such as the medium depth, pulse width, and the medium dispersion strength.

DOI: [10.1103/PhysRevE.91.033206](https://doi.org/10.1103/PhysRevE.91.033206)

PACS number(s): 41.20.Jb, 42.25.Bs, 42.50.Gy, 42.65.An

I. INTRODUCTION

The spectral components comprising an electromagnetic pulse in a temporally dispersive medium are nonuniformly scaled and time shifted during propagation. In general, this leads to pulse envelope reshaping (or distortion). Nevertheless, given the dispersion characteristics of a medium, one can design the wavelength and spectral width of the input pulse so the interference among the spectral components leads to interesting observations, in which the peak of the output pulse evolves at earlier time instants compared to its counterpart in vacuum (with minimum distortion); implying superluminal propagation. In other extreme cases, the pulse peak can even evolve at the output before the peak of the input pulse interacts with the medium, implying a negative group delay. Superluminal group delay and negative group delay refer to the same phenomenon, but from different frames of reference, and are collectively referred-to as abnormal group delay (AGD). The fundamental rules governing AGD are now well established and can be attributed to spectral reshaping [1–12] and energy exchange between the medium and the propagating pulse [13,14].

Many experiments at optical frequencies have demonstrated the possibility of achieving AGD using inverted media with gain doublets [15–19]. In all such cases, it has been confirmed that the earliest response of the medium occurs after a strictly luminal duration equal to (L/c) in compliance with the fundamental requirements of Einstein causality; where L is the medium length and c is the speed of light in vacuum. In such experiments, the fact that the bandwidth of the AGD region is finite over a portion of the input spectrum implies that there always exists a cutoff distance (z_{cutoff}) beyond which a superluminal pulse becomes subluminal. To the best of our knowledge, there is no closed-form expression in the literature by which z_{cutoff} can be directly calculated. In previous efforts the cutoff distance was only calculated numerically [20] and, hence, the exact order dependency of z_{cutoff} on parameters such as the input pulse width and dispersion characteristics remained unexplored.

The goal of this paper is, first, to derive a *simple* closed-form expression to predict the cutoff distance beyond which a superluminal pulse—in a double-resonance gain medium—becomes subluminal. The accuracy of the obtained expression

is tested versus the exact calculations in the frequency domain. Furthermore, the expression quantifies the dependence of the cutoff distance on the characteristics of the input pulse and the medium parameters. This is useful for understanding the capabilities and the design constraints of a broad class of systems that utilize superluminal propagation.

Second, using the saddle-point analysis (method of steepest descent), a superluminal pulse is decomposed into its superluminal and subluminal components. By tracking the evolution of these components under different medium lengths, the physical mechanisms for the transition of a superluminal pulse to a subluminal are explained in light of the derived closed-form expression. Hence, the accuracy of z_{cutoff} expression is tested in the time domain as well.

This paper is organized as follows: in Sec. II, we introduce the dispersive medium considered in our analysis and we present the closed-form expression that predicts the superluminal-to-subluminal cutoff distance. The accuracy of the derived expression is then tested versus the exact calculations. The fundamental limitations of superluminal propagation in light of factors such as the medium depth, pulse width, and the medium dispersion strength are thus discussed. Afterwards, in Sec. III, we present a brief overview on the steepest-descent method used to calculate the evolution of an electromagnetic pulse traveling in a temporally dispersive gain doublet. In Sec. IV, we discuss the time-frequency evolution of an electromagnetic pulse as a result of varying the medium length and highlight the effects of the medium length on superluminal propagation. Finally, Sec. V contains our concluding remarks.

II. DOUBLE-RESONANCE LORENTZIAN MEDIA WITH GAIN

We consider a dispersive medium with AGD in the flat region between a gain doublet. Such a medium can be realized using the gain line of ammonia vapor at the wavelength of a Rb laser (780 nm). The index of refraction for such an inverted medium is described by a double-resonance Lorentzian gain function as follows [21]:

$$n(\omega) = \sqrt{1 + \frac{\omega_{p,1}^2}{\omega^2 - \omega_{0,1}^2 + 2i\delta\omega} + \frac{\omega_{p,2}^2}{\omega^2 - \omega_{0,2}^2 + 2i\delta\omega}}, \quad (1)$$

TABLE I. Numerical values for the parameters of the double-resonance Lorentzian medium with gain (ammonia vapor cells).

$\omega_{0,1}$	2.4165825×10^{15} rad/s
$\omega_{0,2}$	2.4166175×10^{15} rad/s
$\omega_{p,1}$	10×10^9 rad/s
$\omega_{p,2}$	10×10^9 rad/s
δ	2.5×10^9 rad/s

where $\omega_{p,j}$ and $\omega_{0,j}$ ($j = 1$ or 2) are the plasma and resonance frequencies associated with the first and second resonances and δ denotes the phenomenological linewidth. For each resonance, the typical condition $\delta < \omega_{p,j} < \omega_{0,j}$ is satisfied. Such a medium has a causal response and, consequently, the Kramers-Kronig relations are satisfied. The numerical values for the Lorentzian medium parameters are listed in Table I. A similar configuration has been considered in a previous study in order to investigate the speed of information transfer in superluminal channels with different detection noise levels [12]. Here we are rather interested in setting the fundamental limits on the medium length and dispersion characteristics so superluminal propagation can take place.

The real and imaginary parts of the index of refraction $n(\omega)$ are plotted in Fig. 1, where the separation between the medium resonances is in the order of 5 (GHz). For the input excitation we consider a causal Gaussian pulse at $\lambda = 780$ nm ($\omega_c = 2.4166 \times 10^{15}$ rad/s). The input pulse is then given by

$$f(t) = e^{-\frac{t-t_0}{T}} \sin(\omega_c t). \quad (2)$$

The pulse is excited at the $z = 0$ plane and is centered at $t_0 \sim 3T$. The initial spectrum for $f(t)$ is written as

$$F(\omega) = \sqrt{\pi} T e^{-\frac{T^2(\omega-\omega_c)^2}{4}} e^{i(\omega-\omega_c)T_0}. \quad (3)$$

For such an input pulse—with an initial spectrum that is well fitted within the gain doublet—a superluminal effect (group velocity) can be observed over finite propagation distances. However, a superluminal-to-subluminal transition can still

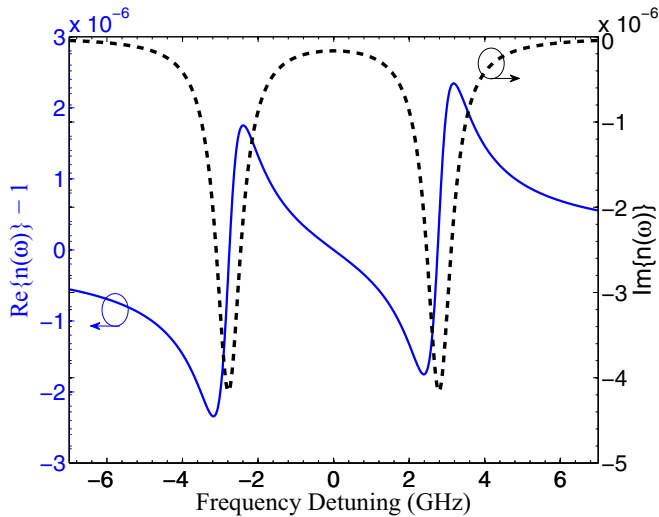


FIG. 1. (Color online) Index of refraction as a function of detuning, the left axis represents the real part and the right axis represents the imaginary part of $n(\omega)$.

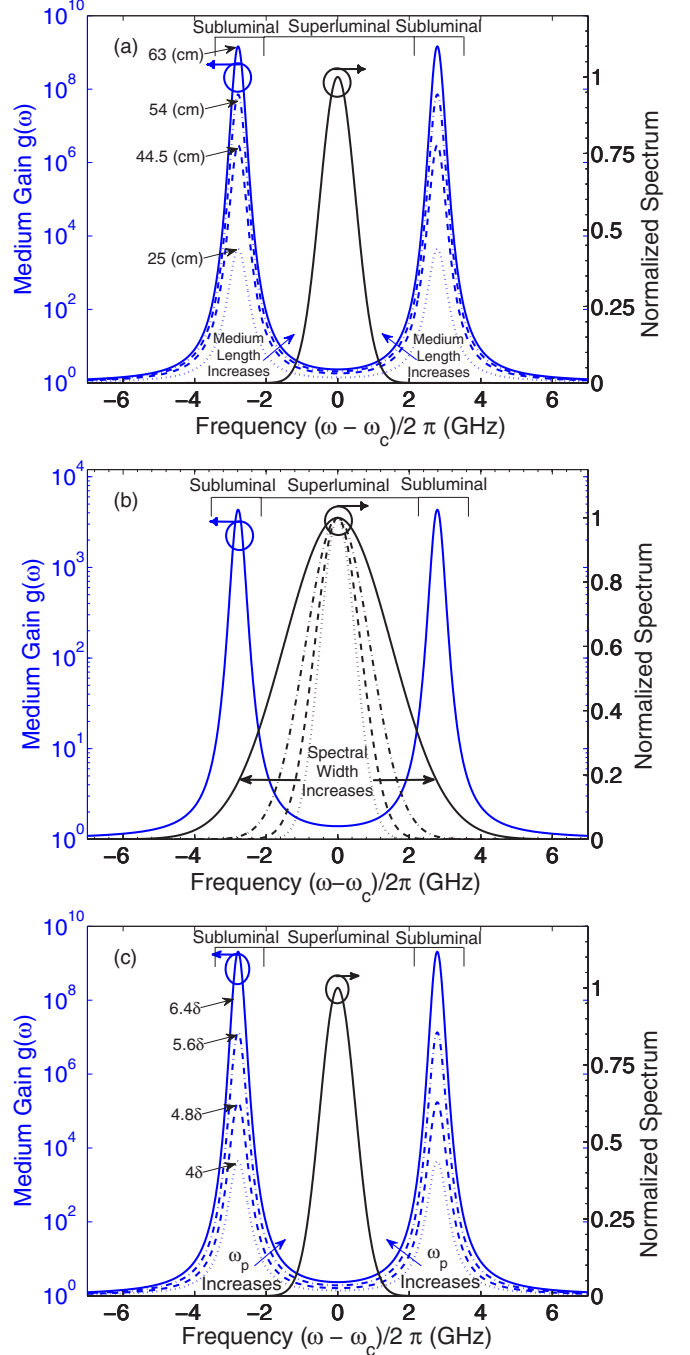


FIG. 2. (Color online) Spectral width and medium gain. (a) The medium gain $g(\omega)$ for $L = 25$ (cm), 44.5 (cm), 54 (cm), and 63 (cm) and a Gaussian pulse width $2T = 0.9$ (ns). (b) Medium gain $g(\omega)$ for $L = 25$ (cm) and pulse widths $2T = 0.9$ (ns), 0.7 (ns), 0.5 (ns), and 0.3 (ns), respectively. (c) The medium gain $g(\omega)$ at a fixed length $L = 25$ (cm) and pulse width $2T = 0.9$ (ns) for oscillator strengths ω_p equal to 4δ , 4.8δ , 5.6δ , and 6.4δ .

take place if the pulse propagates far enough in the medium or if the medium dispersion parameters are tuned [20]. This transition can be attributed to the subluminal components that dominate over the pulse at longer propagation distance. For instance, Fig. 2(a) depicts the input pulse spectrum over the medium gain at four different propagation distances. As the

propagation distance increases, the overlap region between the (subluminal) gain doublet and the initial pulse spectrum expands (as marked by the arrows). Accordingly, the pulse spectrum is no longer confined within the superluminal (flat) region of the medium and is dominated by the *amplified* subluminal components.

Likewise, for a fixed propagation distance, there exists a Gaussian pulse (centered at the superluminal region) with a cutoff spectral width beyond which the pulse becomes subluminal, as depicted in Fig. 2(b). In that case, the gain doublet is fixed and the pulse spectrum leaks outside the superluminal region. Consequently, the overlap region with the subluminal part is expanded and the center of mass of the pulse is delayed.

Additionally, it should be noted that the medium dispersion strength, denoted by the plasma frequency (ω_p), plays an important role that is analogous to the medium depth. For instance, increasing the oscillator strength, ω_p , for both resonances (at a fixed medium depth) yields a behavior that is illustrated in Fig. 2(c). In analogy with the cases discussed in Figs. 2(a) and 2(b), there exists a value for ω_p beyond which a superluminal pulse becomes dominated by its subluminal components as a consequence of the interaction with the gain doublet.

Therefore, the interplay between factors such as the pulse width, propagation depth, and oscillator strength impose fundamental constraints on the propagation distance over which a superluminal effect can be observed. In this paper, we show that for the broad class of dispersive media with gain (that follow a double-resonance Lorentzian function), the interplay between the aforementioned factors can be governed (to a certain degree of accuracy) through the following *approximate* closed-form expression [22]:

$$z_{\text{cutoff}} \approx \frac{c\delta(\omega_{0,2} - \omega_{0,1})^2 T^2}{4\omega_p^2}. \quad (4)$$

The detailed derivation of this expression is provided in the Appendix. Equation (4) governs the relation between the pulse width and the characteristics of the medium (in terms of the dispersion strength, linewidth, and length) and their effect on superluminal propagation.

In order to validate the accuracy of Eq. (4), the obtained cutoff distances are compared with the exact calculations over a wide range of parameters for the input pulse and the medium. The exact calculations of the cutoff distance are performed by evaluating the *arrival time* of the pulse at different values for the medium length, dispersion strength, and input pulse widths. The arrival time is calculated by a procedure that follows directly from Ref. [11]. This involves an averaging of the group delay weighted by the output pulse spectrum as described by

$$\langle t_f \rangle = \frac{\int_{\omega_1}^{\omega_2} \tau_g g(\omega) \mathbf{F}(\omega) d\omega}{\int_{\omega_1}^{\omega_2} g(\omega) \mathbf{F}(\omega) d\omega}, \quad (5)$$

where τ_g is the group delay, $g(\omega)$ is the medium gain, and $F(\omega)$ is the input pulse spectrum obtained from Eq. (3). The subscript f in $\langle t_f \rangle$ denotes that the arrival time is calculated using a frequency domain analysis. By comparing the arrival time obtained from Eq. (5) with the strictly luminal delay

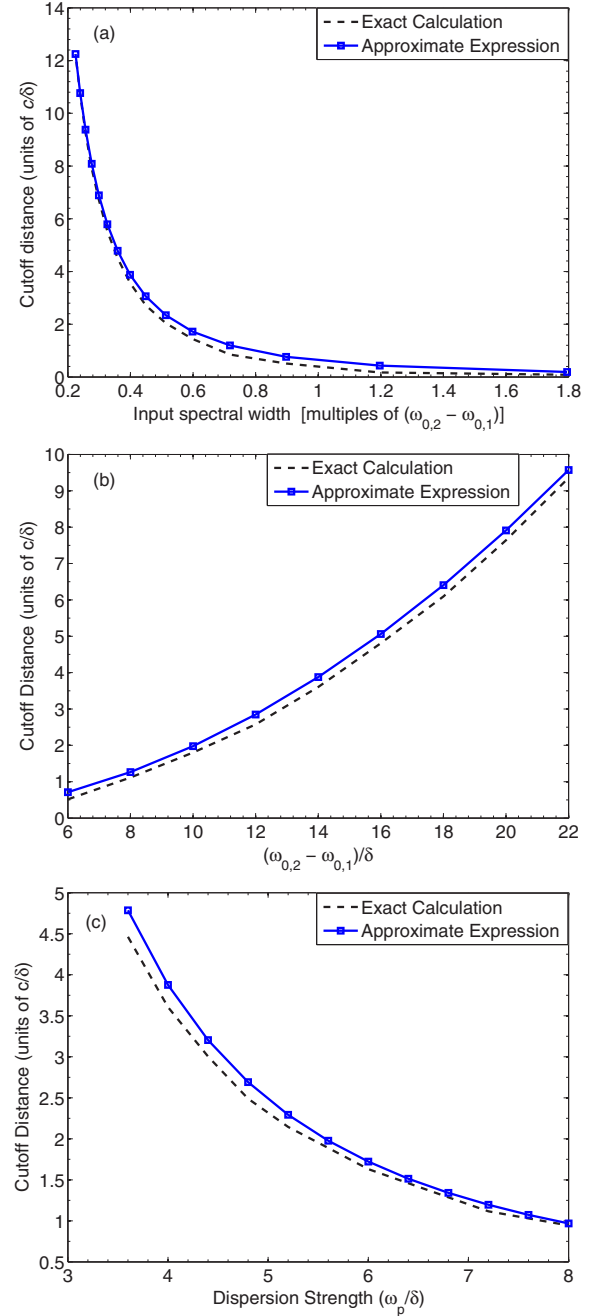


FIG. 3. (Color online) Comparison between the exact calculations of the cutoff distance versus the approximate closed form expression when: (a) The input spectral width is increased (or as the temporal pulse width is reduced). (b) The medium resonances ($\omega_{0,2} - \omega_{0,1}$) are tuned. (c) The plasma frequency (dispersion strength) is increased.

(L/c) over a wide range of propagation distances, one can then deduce the exact cutoff distance at which the superluminal-to-subluminal pulse transition occurs. The comparisons between the approximate expression and the exact calculations are depicted in Fig. 3.

The cutoff distances predicted from Eq. (4) demonstrate a very good agreement with the exact calculations—with a maximum deviation of 5%. In fact, it can be shown that the

expression in Eq. (4) provides an asymptotic upper bound for the cutoff distance. Such expression is quite accurate as long as $\delta < \frac{\omega_{0,2} - \omega_{0,1}}{10}$ and $(\omega_{0,2} - \omega_{0,1}) < \frac{\omega_{0,1}}{10}$, which are typically the case in practice.

Equation (4) captures the physical dynamics involved in the problem in a very compact form; it can be inferred that—for superluminal pulses with larger temporal width (T) (narrow band pulses)—the transition to the subluminal region occurs at a longer cutoff distance (z_{cutoff}) as depicted in Fig. 3(a). This also applies to a double-resonance medium with a wide frequency band between resonances (larger $\omega_{0,2} - \omega_{0,1}$) or a larger linewidth (δ), in which cases the transition occurs at longer propagation distances—as shown in Fig. 3(b). On the other hand, a superluminal pulse propagating in a medium with strong dispersion (larger value for ω_p) would evolve to the subluminal regime at a shorter cutoff distance (z_{cutoff}), as depicted in Fig. 3(c). Finally, it can be inferred from the higher-order dependencies in Eq. (4) that the transition from superluminal to subluminal is more sensitive to the variations in the pulse width (T), frequency detuning ($\omega_{0,2} - \omega_{0,1}$), and dispersion strength (ω_p)—all of which have a quadratic dependency— as compared to the variations in the linewidth (δ).

In this section, we presented a closed-form analytic expression for the cutoff distance at which superluminal-to-subluminal pulse transition occurs. Using this expression, the cutoff distance can be calculated without the need to know the exact spectral distribution of the input pulse. The knowledge of the initial pulse width (T) is sufficient in such calculation. The expression has been verified by comparison with the exact frequency domain calculations. In the following sections, we calculate the temporal evolution of the field at different propagation distances to verify the approximate expression for the cutoff in the time domain. This also gives insight about the time-frequency dynamics that governs the superluminal-to-subluminal transition. In order to do so, the method of steepest descent is incorporated, as discussed next.

III. STEEPEST-DESCENT ANALYSIS FOR PULSE PROPAGATION IN A LORENTZIAN MEDIUM WITH GAIN

The general description of the field $E(z, t)$ is obtained by solving the integral

$$E(z, t) = \frac{1}{2\pi} \text{Re} \left[i \int \tilde{F} e^{z\phi(\omega, \theta')/c} d\omega \right]. \quad (6)$$

The term \tilde{F} describes the spectral amplitude and is expressed as

$$\tilde{F} = \sqrt{\pi} T e^{-i\omega_c t_0}, \quad (7)$$

and the phase term in Eq. (6), $[\phi(\omega, \theta')]$ is given by

$$\phi(\omega, \theta') = i\omega[n(\omega) - \theta'] - \frac{cT^2}{4z}(\omega - \omega_c)^2, \quad (8)$$

where θ' is the dimensionless space-time parameter expressed as $\theta' = c(t - t_0)/z$ and maps to different time instants (given a fixed length z) [23,24].

By following the approach outlined in Ref. [12], the integration contour is carried over the real frequency axis or any other contour that is homotopic to this axis. As such, the output response of the medium is evaluated by adding

the contributions of the saddle-point frequencies (ω_{SP}) that satisfy $\frac{d\phi(\omega=\omega_{\text{SP}}, \theta')}{d\omega} = 0$. This is equivalent to deforming the integration contour along the path of the steepest descent of $\phi(\omega, \theta')$. At each value of θ' , the contribution of each saddle-point frequency—denoted as $A_{\omega_{\text{SP}}}$ —towards the construction of the total field can be expressed in a closed form as [23]

$$A_{\omega_{\text{SP}}}(\theta') = \sqrt{\frac{c}{2\pi z}} \text{Re} \left[\frac{i \tilde{F} e^{z\phi(\omega_{\text{SP}}, \theta')}}{\sqrt{\frac{-d^2}{d\omega^2} \phi(\omega_{\text{SP}}, \theta')}} \right]. \quad (9)$$

In order to calculate the total field response, the contribution of each of the saddle points are added. Accordingly, the asymptotic description of the total field is

$$A_{\text{Total}}(\theta') = \sum_{i=1}^n A_{\omega_{\text{SP}_i}}(\theta'). \quad (10)$$

The method of steepest descent thus can be used to evaluate (and assess the significance of) the different spectral components of the pulse (part of which may be superluminal or subluminal). In the next section, we apply the method of steepest descent to a pulse propagating in the medium expressed in Eq. (1) to study the evolution of its subluminal and superluminal components at longer propagation distances in light of the expression of Eq. (4). Accordingly, the physical mechanism of the superluminal-to-subluminal transition is demonstrated.

IV. PHYSICAL DYNAMICS OF A SUPERLUMINAL PULSE AT LONGER PROPAGATION LENGTHS

In this section, we consider a Gaussian pulse given by Eq. (2), propagating in a double Lorentzian medium [Eq. (1)]. The behavior of the pulse is compared at four different propagation lengths. As discussed in Sec. III, the total field is calculated by adding the contributions of the saddle-point frequencies that satisfy $\frac{d\phi(\omega=\omega_{\text{SP}}, \theta')}{d\omega} = 0$. The exact locations of the saddle points are numerically calculated at each instant of time (θ') and are plotted in Fig. 4. The four subplots [Figs. 4(a)–4(d)] correspond to propagation distances (L) equal to 25 (cm), 44.5 (cm), 54 (cm), and 63 (cm), respectively. The first and second resonances of $n(\omega)$ are denoted by $(\omega_{0,1})$ and $(\omega_{0,2})$, respectively. The terms $(\omega_+^{(0)}, \omega_+^{(1)})$ and $(\omega_+^{(2)}, \omega_+^{(3)})$ signify the branch cuts for $n(\omega)$. The frequency ranges that correspond to the superluminal and the subluminal regions are shown in the same figure. The arrows depict the path of the dominant saddle points, which are labeled $\omega_{\text{SP},M}$, $\omega_{\text{SP},L}$, and $\omega_{\text{SP},R}$. Clearly, the saddle-point paths exhibit a symmetry about the carrier frequency ω_c . Moreover, it is found that at each instant of θ' , the contribution of the saddle-point frequencies, $\omega_{\text{SP},M}$, $\omega_{\text{SP},L}$, and $\omega_{\text{SP},R}$, are much more pronounced than the other two saddle points below the branch cuts. As such, the integration contour is deformed along the steepest-descent path in the upper half complex plane of $\phi(\omega, \theta')$.

For a pulse with an initial spectrum *well fitted* within the superluminal region such as the one considered in Fig. 4(a), it will be shown that the output field is *dominated* by the contributions of the middle saddle points, $\omega_{\text{SP},M}$, which follow a vertical path downwards at the carrier frequency in the middle of the *superluminal* region. The other saddle points,

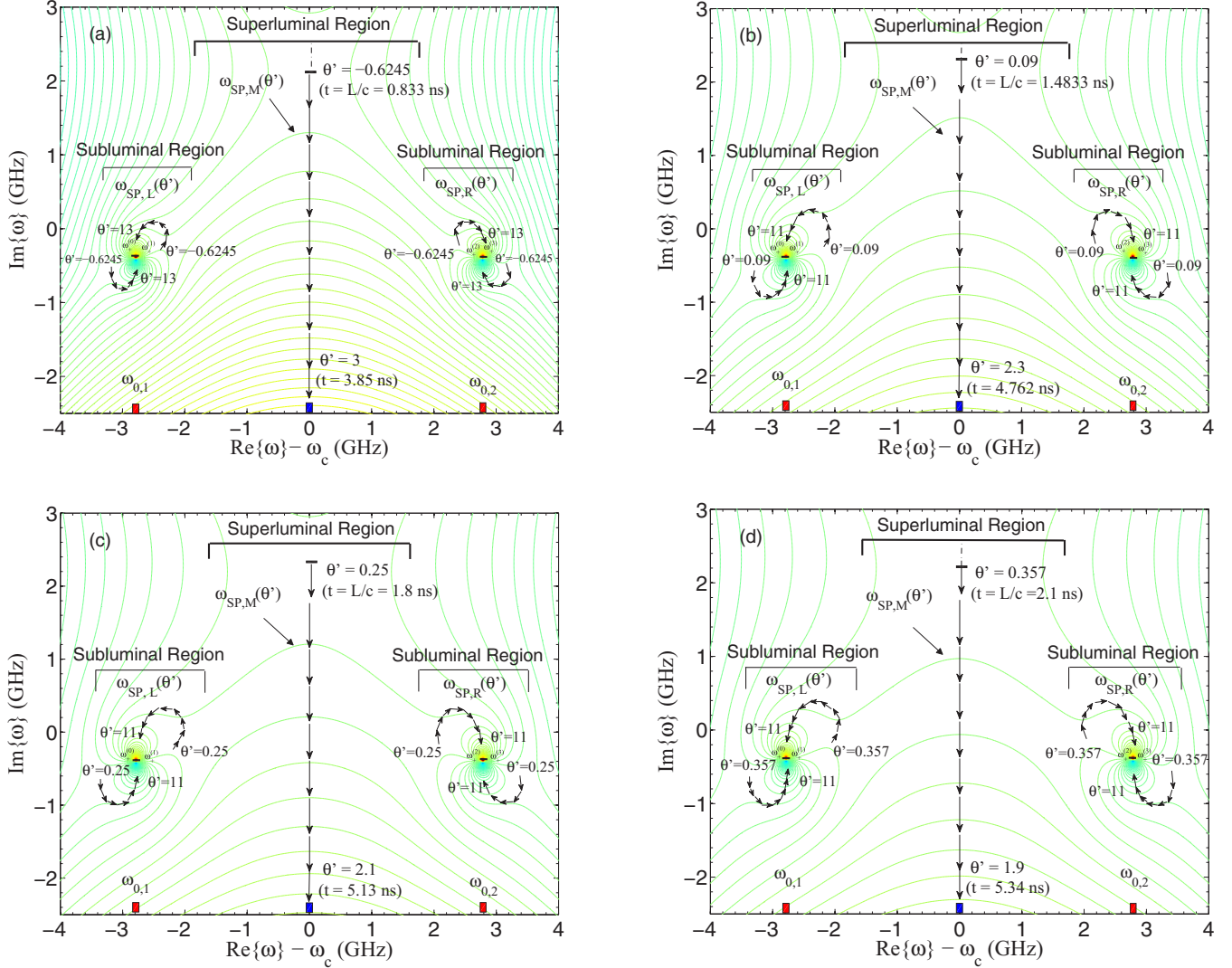


FIG. 4. (Color online) Subplots (a)–(d) correspond to propagation lengths of 25, 44.5, 54, and 63 (cm) inside the ammonia vapor cells, respectively. The arrows show the path of the saddle points in the complex frequency domain. The colored (green) contours show the real part of the phase function $[\text{Re}\{\phi(\omega, \theta')\}]$ for $t = L/c$.

$\omega_{\text{SP},L}$ and $\omega_{\text{SP},R}$, both of which lie in the subluminal frequency region, have minimal contributions to the construction of the total field. As the pulse further penetrates inside the medium, the interaction of the pulse side bands with the gain doublet becomes more pronounced. This is evident in cases (b) through (d) [Figs. 4(b)–4(d)] in which the circular path of the saddle points, $\omega_{\text{SP},L}$ and $\omega_{\text{SP},R}$, becomes more spread out around the branch cuts at longer propagation depths. As the radius of this circular path increases, approaching the carrier frequency ω_c , the contributions of the corresponding (*subluminal*) saddle points become more significant. It is worth noting that a larger saddle-point path (at longer propagation distance) corresponds to wider range of (*subluminal*) frequencies in the spectral content of the signal. It is the amplification of these (*subluminal*) frequencies that leads to the superluminal-to-subluminal pulse transition.

In all cases (a)–(d) [Figs. 4(a)–4(d)], the path direction of the saddle points located in the subluminal region, $\omega_{\text{SP},L}$ and $\omega_{\text{SP},R}$, implies that not only is the contribution of the saddle

points significantly delayed with respect to the superluminal component of the pulse (associated with $\omega_{\text{SP},M}$), but it suffers from chirping as well. For the path of $\omega_{\text{SP},L}$, the instantaneous frequency is decreasing in the direction of the branch cut ($\omega_+^{(0)}, \omega_+^{(1)}$), whereas for the path of $\omega_{\text{SP},R}$, the instantaneous frequency is increasing in the direction of the other branch cut ($\omega_+^{(2)}, \omega_+^{(3)}$).

By direct substitution in Eq. (9), the contributions of $\omega_{\text{SP},M}$, denoted as $A_{\omega_{\text{SP},M}}(\theta')$ and the contributions of $\omega_{\text{SP},L}$, denoted as $A_{\omega_{\text{SP},L}}(\theta')$, are plotted in Figs. 5(a)–5(d). The contributions of $\omega_{\text{SP},R}$ maintain a close resemblance with the contributions of $\omega_{\text{SP},L}$ and are not included in the plots for the sake of brevity. The corresponding saddle points are represented by the dotted line and the direction of their path is marked by the black arrows. Accordingly, at each instant of time (θ'), the instantaneous fields are mapped to their corresponding saddle-point frequencies on the same plot. It is worth noting that the path of $\omega_{\text{SP},R}$ would exhibit a symmetry about the horizontal frequency axis with $\omega_{\text{SP},L}$ path.

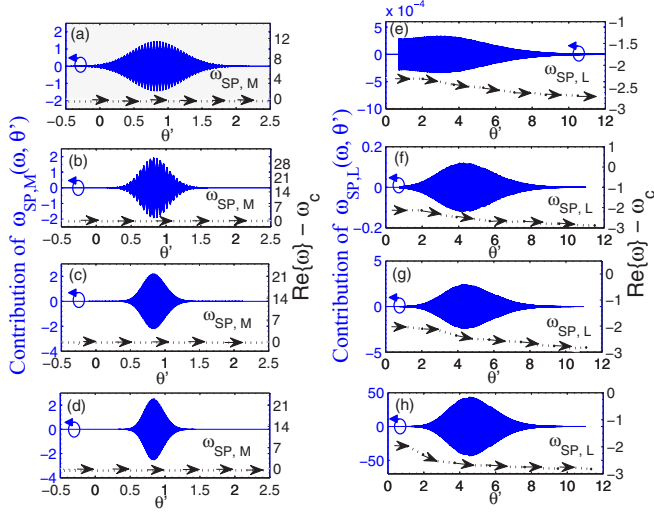


FIG. 5. (Color online) Saddle-point contributions. The dotted lines represent the path of the saddle points ($\omega_{SP,M}$ and $\omega_{SP,L}$). The left column corresponds to the contributions of $\omega_{SP,M}$ and the right column corresponds to the contributions of $\omega_{SP,L}$. Cases [(a)–(e), (b)–(f), (c)–(g), and (d)–(h)] refer to propagation lengths of 25, 44.5, 54, and 63 (cm) inside the ammonia vapor cells, respectively.

As the propagation length increases from 25 to 63 cm, the superluminal component—associated with $\omega_{SP,M}$ —experiences slight amplification and compression. On the other hand, the subluminal components associated with $\omega_{SP,L}$ and $\omega_{SP,R}$ experience broadening and are more significantly amplified. Since the rate of amplification for the subluminal components is much more significant than the rate of amplification for the superluminal component, the output pulse is no longer dominated by the superluminal component at longer propagation distances. This behavior is generic and represent a duality with passive media in which the rate of absorption in the superluminal region is much more pronounced as compared to the absorption encountered in the subluminal region [25].

The total field is evaluated and plotted in Figs. 6(a)–6(d) by adding the contributions of all the saddle points. The dashed lines refer to the case of a companion pulse traveling the same distance in vacuum for comparison. In order to quantitatively characterize the arrival time for the pulses propagating in the AGD medium, as compared to their counterpart in vacuum, the center of mass of the pulse is calculated. The arrival time *expectation* denoted as $\langle t \rangle$ is listed for cases (a)–(d) in Figs. 6(a)–6(d) and is expressed as follows [11,20]:

$$\langle t \rangle = \frac{\hat{u} \cdot \int_{-\infty}^{\infty} t \mathbf{S}(\mathbf{z}, t) dt}{\hat{u} \cdot \int_{-\infty}^{\infty} \mathbf{S}(\mathbf{z}, t) dt}. \quad (11)$$

The term $\mathbf{S}(\mathbf{z}, t)$ denotes the Poynting vector of the propagating field and \hat{u} is a unit vector along the normal direction to the detector surface. This product becomes significant in angularly dispersive media where the numerator and denominator of Eq. (11) are not necessarily in parallel directions (which is not the case in this analysis).

Figure 6 shows that the pulse, after propagating for 25 (cm) in the AGD medium, exhibits time advancement as compared to the companion pulse in vacuum. This is attributed to the

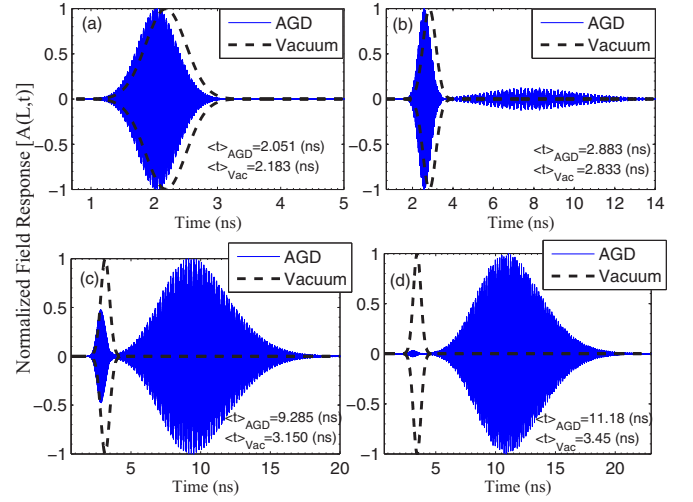


FIG. 6. (Color online) The total output field $A(L, t)$. The black dotted curves correspond to the case of vacuum and $\langle t \rangle$ denotes the pulse arrival time. Cases (a)–(d) refer to propagation lengths of 25, 44.5, 54, and 63 (cm), respectively.

fact that the superluminal components are dominant at this propagation distance, as previously discussed. However, at longer penetration depths, cases (b) through (d) [Figs. 6(b)–6(d)], the subluminal components become more pronounced and the pulse in the AGD medium is delayed as compared to the companion pulse in vacuum. This implies that the center of mass for a superluminal pulse is delayed after propagating for distances longer than ~ 43 cm, in agreement with the expression in Eq. (4).

Moreover, the transition of a superluminal pulse to a subluminal—in an inverted medium—is usually accompanied with pulse broadening. For a Gaussian excitation, the pulse width is proportional to the variance and can be described as $\sigma^2 = [\langle t^2 \rangle - \langle t \rangle^2]$ [20]. The pulse broadening factor, Γ , can be expressed as

$$\Gamma = \frac{[\langle t^2 \rangle - \langle t \rangle^2]_{AGD}}{[\langle t^2 \rangle - \langle t \rangle^2]_{Vac}}. \quad (12)$$

From the definition in Eq. (12), intervals within which $\Gamma < 1$ implies pulse compression, while $\Gamma > 1$ implies pulse broadening. For the cases (a)–(d) [Figs. 6(a)–6(d)] considered in this section, the pulse broadening factor Γ is equal to 0.9323, 32.15, 99.93, and 68.972, respectively. Pulse broadening can be attributed to the fact that the spectral components that lie within the subluminal region experience larger gain and differential delay. It is concluded that pulse broadening always precedes the transition of a superluminal pulse to the subluminal regime.

In this section, the time-frequency dynamics associated with superluminal pulse transition to a subluminal regime (at longer propagation distances) has been presented. Furthermore, the superluminal-to-subluminal cutoff distance predicted in Eq. (4) has been verified. A similar analysis can be extended for input pulses with narrower temporal widths and media with stronger dispersion strengths to reach the same conclusions governed by Eq. (4).

V. CONCLUSION

In this paper, we have presented a simple closed-form analytic expression to predict the cutoff distance at which a superluminal pulse becomes subluminal. The expression provides the fundamental limitations of superluminal pulse propagation in light of factors such as the propagation distance, pulse spectrum, and medium dispersion strength. Furthermore, the method of steepest descent has been utilized to investigate the time-frequency dynamics associated with the transition from the superluminal to the subluminal regime, in an inverted medium. This has been done by decomposing a superluminal pulse into its superluminal and subluminal components under different configurations. Cases in which a superluminal pulse evolves to the subluminal regime at longer propagation depths have been presented to verify the approximate analytic expression. This evolution is attributed to the subluminal spectral components that dominate over the pulse during propagation.

ACKNOWLEDGMENT

This work was supported by the Natural Sciences and Engineering Research Council of Canada (NSERC-CREATE Program) under Grant No. CREATE 371066-09.

APPENDIX: DERIVATION OF Z_{cutoff}

In this Appendix, the equation for the cutoff distance— at which a superluminal Gaussian pulse becomes subluminal— in an inverted medium is derived. By calculating the energy content of the subluminal component and comparing it with the superluminal energy content of the pulse and performing the formulation as a function of the medium length, one can derive an expression for the cutoff distance at which the superluminal and subluminal energy components are equal.

The double-resonance gain medium considered in the analysis is given by

$$n(\omega) = \sqrt{1 + \frac{\omega_{p,1}^2}{2i\delta\omega + \omega^2 - \omega_{0,1}^2} + \frac{\omega_{p,2}^2}{2i\delta\omega + \omega^2 - \omega_{0,2}^2}}. \quad (\text{A1})$$

$$\text{Im} \left\{ n \left(\frac{\omega_{0,1} + \omega_{0,2}}{2} \right) \right\} = \frac{1}{2} \delta(\omega_{0,1} + \omega_{0,2}) \left\{ - \frac{\omega_{p,1}^2}{\delta^2(\omega_{0,1} + \omega_{0,2})^2 + [\omega_{0,1}^2 - \frac{1}{4}(\omega_{0,1} + \omega_{0,2})^2]^2} - \frac{\omega_{p,2}^2}{\delta^2(\omega_{0,1} + \omega_{0,2})^2 + [\omega_{0,2}^2 - \frac{1}{4}(\omega_{0,1} + \omega_{0,2})^2]^2} \right\}. \quad (\text{A6})$$

In order to calculate the gain in the subluminal region, we first evaluate $\omega_{0,1} \times \text{Im}\{n(\omega_{0,1})\}$ [or, equivalently, $\omega_{0,2} \times \text{Im}\{n(\omega_{0,2})\}$] since the only change between the two expressions is substituting $\omega_{0,1}$ for $\omega_{0,2}$ and simplify the resulting expression to get

$$\omega_{0,1} \times \text{Im}\{n(\omega_{0,1})\} = - \frac{\delta\omega_{0,1}^2\omega_{p,2}^2}{4\delta^2\omega_{0,1}^2 + (\omega_{0,1}^2 - \omega_{0,2}^2)^2} - \frac{\omega_{p,1}^2}{4\delta}. \quad (\text{A7})$$

For this case, the approximation ($\sqrt{1+x} \approx 1+x/2$) holds and, thus, $n(\omega)$ can be rewritten as follows:

$$n(\omega) = 1 + \frac{1}{2} \left(\frac{\omega_{p,1}^2}{2i\delta\omega + \omega^2 - \omega_{0,1}^2} + \frac{\omega_{p,2}^2}{2i\delta\omega + \omega^2 - \omega_{0,2}^2} \right). \quad (\text{A2})$$

Accordingly, the imaginary part of $n(\omega)$ is written as

$$n_i(\omega) = -i\delta\omega \left[\frac{\omega_{p,1}^2}{4\delta^2\omega^2 + (\omega^2 - \omega_{0,1}^2)^2} + \frac{\omega_{p,2}^2}{4\delta^2\omega^2 + (\omega^2 - \omega_{0,2}^2)^2} \right]. \quad (\text{A3})$$

Furthermore, the medium gain is expressed [as a function of ω , z , and $n(\omega)$] by $g(\omega) = e^{-\omega \text{Im}\{n(\omega)\}z/c}$. In order to derive the ratio between the gain associated with the subluminal and superluminal components, we calculate the medium gain in the corresponding frequency regions. For the subluminal region, the maximum gain typically occurs at the position of the resonance frequency ($\omega_{0,i}$); as such, the imaginary component of $n(\omega)$, evaluated at ($\omega_{0,1}$), is given by

$$\text{Im}\{n(\omega_{0,1})\} = - \frac{\delta\omega_{0,1}\omega_{p,2}^2}{4\delta^2\omega_{0,1}^2 + (\omega_{0,1}^2 - \omega_{0,2}^2)^2} - \frac{\omega_{p,1}^2}{4\delta\omega_{0,1}}. \quad (\text{A4})$$

Similarly,

$$\text{Im}\{n(\omega_{0,2})\} = - \frac{\delta\omega_{0,2}\omega_{p,1}^2}{4\delta^2\omega_{0,2}^2 + (\omega_{0,1}^2 - \omega_{0,2}^2)^2} - \frac{\omega_{p,2}^2}{4\delta\omega_{0,2}}. \quad (\text{A5})$$

As for the gain in the superluminal region (which is typically centered between the two resonances), the imaginary component of $n(\omega)$ can be expressed as

By replacing $\omega_{0,2}$ with $\omega_{0,1} + \Delta$, and ignoring any higher-order nonlinear terms in Δ , Eq. (A7) can be simplified to

$$\omega_{0,1} \times \text{Im}\{n(\omega_{0,1})\} = - \frac{\omega_{p,2}^2}{4\delta\Delta^2} - \frac{\omega_{p,1}^2}{4\delta}. \quad (\text{A8})$$

However, since usually $\frac{\omega_{p,2}^2}{4\delta\Delta^2} \ll \frac{\omega_{p,1}^2}{4\delta}$, this can be further simplified to

$$\omega_{0,1} \times \text{Im}\{n(\omega_{0,1})\} \approx - \frac{\omega_{p,1}^2}{4\delta}. \quad (\text{A9})$$

Similarly, we can get

$$\omega_{0,2} \times \text{Im}\{n(\omega_{0,2})\} \approx -\frac{\omega_{p,2}^2}{4\delta}. \quad (\text{A10})$$

In most practical cases, the values for $\omega_{p,1}$ and $\omega_{p,2}$ are very close in order to maintain a flat region between the gain doublets. Furthermore, the frequency detuning between the resonances ($\omega_{0,1}$ and $\omega_{0,2}$) is sufficiently close so we may account for the gain of either resonance in terms of the averaged value for $\omega \text{Im}\{n(\omega)\}$. Accordingly, the following expression may be used instead of Eqs. (A9) and (A10) to calculate the gain in the subluminal region:

$$\omega_{0,i} \times \text{Im}\{n(\omega_{0,i})\} = -\frac{\omega_{p,2}^2 + \omega_{p,1}^2}{8\delta}. \quad (\text{A11})$$

This approximation is valid as long as $\omega_{0,2}$ is not much larger than $\omega_{0,1}$ ($\omega_{0,2} < 10 \times \omega_{0,1}$), which is typically the case in most practical scenarios. Consequently, the gain associated with the subluminal region (for only one resonance) is expressed by

$$g(\omega, z)_{\text{subluminal}} = \exp \left[\left(\frac{\omega_{p,2}^2 + \omega_{p,1}^2}{8\delta} \right) \frac{z}{c} \right]. \quad (\text{A12})$$

To calculate the gain at the superluminal region, we must first evaluate $\frac{\omega_{0,1} + \omega_{0,2}}{2} \times \text{Im}\{n(\frac{\omega_{0,1} + \omega_{0,2}}{2})\}$ and simplify the resulting expression. Consequently, the following equation can be derived:

$$\begin{aligned} \frac{\omega_{0,1} + \omega_{0,2}}{2} \times \text{Im} \left\{ n \left(\frac{\omega_{0,1} + \omega_{0,2}}{2} \right) \right\} &= \frac{1}{4} \delta (\omega_{0,1} + \omega_{0,2})^2 \left\{ -\frac{\omega_{p,1}^2}{\delta^2 (\omega_{0,1} + \omega_{0,2})^2 + [\omega_{0,1}^2 - \frac{1}{4}(\omega_{0,1} + \omega_{0,2})^2]^2} \right. \\ &\quad \left. - \frac{\omega_{p,2}^2}{\delta^2 (\omega_{0,1} + \omega_{0,2})^2 + [\omega_{0,2}^2 - \frac{1}{4}(\omega_{0,1} + \omega_{0,2})^2]^2} \right\}. \end{aligned} \quad (\text{A13})$$

In general, $\delta \ll \omega_{0,i}$ and hence the term $\delta^2 (\omega_{0,1} + \omega_{0,2})^2$ in the denominator is usually ~ 2 orders of magnitude smaller than the other term in the denominator and, as such, can be omitted in both fractions. Accordingly, we get

$$\frac{\omega_{0,1} + \omega_{0,2}}{2} \times \text{Im} \left\{ n \left(\frac{\omega_{0,1} + \omega_{0,2}}{2} \right) \right\} = \frac{1}{4} \delta (\omega_{0,1} + \omega_{0,2})^2 \left\{ -\frac{\omega_{p,1}^2}{[\omega_{0,1}^2 - \frac{1}{4}(\omega_{0,1} + \omega_{0,2})^2]^2} - \frac{\omega_{p,2}^2}{[\omega_{0,2}^2 - \frac{1}{4}(\omega_{0,1} + \omega_{0,2})^2]^2} \right\}. \quad (\text{A14})$$

By replacing the term $\omega_{0,2}$ with $\omega_{0,1} + \Delta$, and ignoring any higher-order nonlinear terms in Δ , Eq. (A14) can be simplified to

$$\frac{\omega_{0,1} + \omega_{0,2}}{2} \times \text{Im} \left\{ n \left(\frac{\omega_{0,1} + \omega_{0,2}}{2} \right) \right\} = \frac{1}{4} \delta (\omega_{0,1} + \omega_{0,2})^2 \left[-\frac{\omega_{p,1}^2}{\omega_{0,1}^2 (\omega_{0,2} - \omega_{0,1})^2} - \frac{\omega_{p,2}^2}{\omega_{0,2}^2 (\omega_{0,2} - \omega_{0,1})^2} \right]. \quad (\text{A15})$$

Thus the gain at the superluminal region can be written in a straightforward manner in the following form:

$$g(\omega, z)_{\text{superluminal}} = \exp \left\{ \frac{1}{4} \delta (\omega_{0,1} + \omega_{0,2})^2 \left[\frac{\omega_{p,1}^2}{\omega_{0,1}^2 (\omega_{0,2} - \omega_{0,1})^2} + \frac{\omega_{p,2}^2}{\omega_{0,2}^2 (\omega_{0,2} - \omega_{0,1})^2} \right] \frac{z}{c} \right\}. \quad (\text{A16})$$

Thus far, we have derived expressions for the gain associated with the superluminal and subluminal regions. In the following, we include the input pulse into the calculations in order to evaluate the corresponding energy content in the superluminal and the subluminal regions. Accordingly, the cutoff distance (at which the energy contents level out) can be derived.

We chose an input-modulated Gaussian excitation with carrier frequency (ω_c) that is centered at $(\frac{\omega_{0,1} + \omega_{0,2}}{2})$. The input pulse envelope is given by $e^{-\frac{1}{4}T^2(\omega - \omega_c)^2}$. We estimate the subluminal region associated with the resonances ($\omega_{0,1}$ and $\omega_{0,2}$) to be extended over the frequency ranges: $[\omega_{0,1} - 3\delta, \omega_{0,1} + 3\delta]$ and $[\omega_{0,2} - 3\delta, \omega_{0,2} + 3\delta]$, respectively. Consequently, the energy content of the input pulse that lies within the subluminal part (for each resonance) is roughly proportional to

$$6\delta e^{-\frac{1}{4}T^2(\omega_{0,1} - \omega_c)^2}. \quad (\text{A17})$$

To account for both resonances, Eq. (A17) is rewritten as

$$12\delta e^{-\frac{1}{4}T^2(\omega_{0,1} - \omega_c)^2}. \quad (\text{A18})$$

The gain experienced by this component has been given in Eq. (A12).

As for the superluminal region, we assume that it extends over the remaining frequency range. The average energy content of the input pulse that lies within the superluminal region is proportional to

$$\frac{1}{2}(-6\delta - \omega_{0,1} + \omega_{0,2}), \quad (\text{A19})$$

where the factor ($\frac{1}{2}$) accounts for averaging the peak value of the Gaussian (centered at the carrier frequency) over the superluminal frequency range. The gain experienced by this component has been given in Eq. (A16).

In order to obtain the cutoff distance at which a superluminal pulse become subluminal, we solve for the distance z at which the energy content associated with the superluminal and subluminal components of the pulse become equal. By scaling the input energy associated with the subluminal component [from Eq. (A18)] by its corresponding gain [obtained in Eq. (A12)] and equating the result with the energy content of the superluminal part [from Eq. (A19)] scaled by the respective

gain [in Eq. (A16)], the following equation can be derived:

$$12\delta \exp \left[\frac{z(\omega_{p,1}^2 + \omega_{p,2}^2)}{8c\delta} - \frac{1}{4}T^2(\omega_{0,1} - \omega_c)^2 \right] = \frac{1}{2}(-6\delta - \omega_{0,1} + \omega_{0,2}) \times \exp \left\{ \frac{\delta(\omega_{0,1} + \omega_{0,2})^2 z \left[\frac{\omega_{p,1}^2}{\omega_{0,1}^2(\omega_{0,1} - \omega_{0,2})^2} + \frac{\omega_{p,2}^2}{(\omega_{0,1} - \omega_{0,2})^2 \omega_{0,2}^2} \right]}{4c} \right\}. \quad (\text{A20})$$

By solving this equation for z , the cutoff distance z_{cutoff} can be expressed as

$$z_{\text{cutoff}} = - \frac{2c\delta\omega_{0,1}^2(\omega_{0,1} - \omega_{0,2})^2\omega_{0,2}^2 [T^2(\omega_{0,1} - \omega_c)^2 + 4 \log \left(- \frac{6\delta + \omega_{0,1} - \omega_{0,2}}{24\delta} \right)]}{2\delta^2(\omega_{0,1} + \omega_{0,2})^2(\omega_{0,2}^2\omega_{p,1}^2 + \omega_{0,1}^2\omega_{p,2}^2) - \omega_{0,1}^2(\omega_{0,1} - \omega_{0,2})^2\omega_{0,2}^2(\omega_{p,1}^2 + \omega_{p,2}^2)}. \quad (\text{A21})$$

In fact, the expression for z_{cutoff} [given in Eq. (A21)] can be further simplified by omitting the term $[\log(-\frac{6\delta + \omega_{0,1} - \omega_{0,2}}{24\delta})]$ in the numerator and the term $[2\delta^2(\omega_{0,1} + \omega_{0,2})^2(\omega_{0,2}^2\omega_{p,1}^2 + \omega_{0,1}^2\omega_{p,2}^2)]$ in the denominator. It can be shown that the contributions of both terms can be neglected [as long as $\delta < \frac{\omega_{0,2} - \omega_{0,1}}{10}$ and $(\omega_{0,2} - \omega_{0,1}) < \frac{\omega_{0,1}}{10}$]. Therefore, Eq. (A21) can be rewritten in the following compact form:

$$z_{\text{cutoff}} \approx \frac{c\delta(\omega_{0,2} - \omega_{0,1})^2 T^2}{4\omega_p^2}. \quad (\text{A22})$$

-
- [1] L. Brillouin, *Wave Propagation and Group Velocity*, Pure and Applied Physics Series (Academic Press, New York, 1960).
- [2] E. L. Bolda, R. Y. Chiao, and J. C. Garrison, Two theorems for the group velocity in dispersive media, *Phys. Rev. A* **48**, 3890 (1993).
- [3] R. Y. Chiao and A. M. Steinberg, Tunneling times and superluminality, *Progr. Opt.* **37**, 345 (1997).
- [4] Klaas Wynne, Causality and the nature of information, *Opt. Commun.* **209**, 85 (2002).
- [5] Zhenshan Yang, Physical mechanism and information velocity of fast light: A time-domain analysis, *Phys. Rev. A* **87**, 023801 (2013).
- [6] G. Diener, Superluminal group velocities and information transfer, *Phys. Lett. A* **223**, 327 (1996).
- [7] M. Mojahedi, E. Schamiloglu, F. Hegeler and K. J. Malloy, Time-domain detection of superluminal group velocity for single microwave pulses, *Phys. Rev. E* **62**, 5758 (2000).
- [8] J. M. W. Mitchell and R. Y. Chiao, Causality and negative group delays in a simple bandpass amplifier, *Am. J. Phys.* **66**, 14 (1998).
- [9] M. Tomita, H. Amano, S. Masegi, and A. I. Talukder, Direct observation of a pulse peak using a peak-removed Gaussian optical pulse in a superluminal medium, *Phys. Rev. Lett.* **112**, 093903 (2014).
- [10] A. Kuzmich, A. Dogariu, L. J. Wang, P. W. Milonni, and R. Y. Chiao, Signal velocity, causality, and quantum noise in superluminal light pulse propagation, *Phys. Rev. Lett.* **86**, 3925 (2001).
- [11] J. Peatross, S. A. Glasgow, and M. Ware, Average energy flow of optical pulses in dispersive media, *Phys. Rev. Lett.* **84**, 2370 (2000).
- [12] Ahmed H. Dorrah, and Mo Mojahedi, Velocity of detectable information in faster-than-light pulses, *Phys. Rev. A* **90**, 033822 (2014).
- [13] J. Peatross, M. Ware, and S. A. Glasgow, Role of the instantaneous spectrum on pulse propagation in causal linear dielectrics, *J. Opt. Soc. Am. A* **18**, 1719 (2001).
- [14] M. Ware, S. A. Glasgow, and J. Peatross, Energy transport in linear dielectrics, *Opt. Express* **9**, 519 (2001).
- [15] L. J. Wang, A. Kuzmich, and A. Dogariu, Gain-assisted superluminal light propagation, *Nature* **406**, 277 (2000).
- [16] M. D. Stenner, D. J. Gauthier, and M. A. Neifeld, The speed of information in a fast-light optical medium, *Nature* **425**, 695 (2003).
- [17] K. Kim, Han Seb Moon, Chunghee Lee, Soo Kyoung Kim, and Jung Bog Kim, Observation of arbitrary group velocities of light from superluminal to subluminal on a single atomic transition line, *Phys. Rev. A* **68**, 013810 (2003).
- [18] J. Keaveney, I. G. Hughes, A. Sargsyan, D. Sarkisyan, and C. S. Adams, Maximal refraction and superluminal propagation in a gaseous nanolayer, *Phys. Rev. Lett.* **109**, 233001 (2012).
- [19] U. Vogl, R. Glasser, and P. Lett, Advanced detection of information in optical pulses with negative group velocity, *Phys. Rev. A* **86**, 031806(R) (2012).
- [20] L. Nanda, H. Wanare, and S. A. Ramakrishna, Why do superluminal pulses become subluminal once they go far enough?, *Phys. Rev. A* **79**, 041806 (2009).
- [21] A. M. Steinberg and R. Y. Chiao, Dispersionless, highly superluminal propagation in a medium with a gain doublet, *Phys. Rev. A* **49**, 2071 (1994).
- [22] The detailed derivation of this equation can be found in the Appendix.
- [23] C. M. Balictsis and K. E. Oughstun, Generalized asymptotic description of the propagated field dynamics in Gaussian pulse propagation in a linear, causally dispersive medium, *Phys. Rev. E* **55**, 1910 (1997).
- [24] R. Safian, M. Mojahedi, and C. D. Sarris, Asymptotic description of wave propagation in an active Lorentzian medium, *Phys. Rev. E* **75**, 066611 (2007).
- [25] Md. A. I. Talukder, Y. Amagishi, and M. Tomita, Superluminal to subluminal transition in the pulse propagation in a resonantly absorbing medium, *Phys. Rev. Lett.* **86**, 3546 (2001).